

UDK 549.67; 622.785

## Characterization of Material Sintered from the Final Flotation Waste and Zeolitic Tuff

Mira Cocić<sup>1\*)</sup>, Mihovil Logar<sup>2</sup>, Viša Tasić<sup>3</sup>, Branko Matović<sup>4</sup>, Milica Miletić-Svirčev<sup>5</sup>

<sup>1</sup>University of Belgrade, Technical Faculty in Bor, VJ 12, 19210 Bor, Serbia

<sup>2</sup>Committee for Geochemistry, Serbian Academy of Sciences and Arts, 11000 Belgrade, Serbia

<sup>3</sup>Mining and Metallurgy Institute Bor, Zeleni bulevar 35, 19210 Bor, Serbia

<sup>4</sup>University of Belgrade, Vinca Institute of Nuclear Sciences, PO Box 522, 11000 Belgrade, Serbia

<sup>5</sup>ALS Laboratory d.o.o., Nikole Kopernika bb 19210 Bor, Serbia

---

### Abstract:

*The paper deals with the characteristics of synthesized glass-ceramics obtained by sintering a mixture of final flotation waste (FFW) with tuff at 1260°C for 7 h, followed by the annealing of pressed samples at 1080°C for 36 h. The experiments were done in order to find the possibility for the valorization of waste material (FFW). By thermal treatment of mixtures of T20 (20 % tuff, 80 % FFW) and T40 (40 % tuff, 60 % FFW) to a temperature of 1260°C over a period of 7 hours, is obtained glass-ceramics with dendritic structure. The synthesized glass-ceramics consists of two phases: iron oxide crystals (maghemite, magnetite, and hematite) and glass with an approximate ratio of phases 32/68 (T20) and 23/77 (T40), respectively. The relatively small shrinkage of the synthesized material (up to 7 %) enables reliable control when designing a given shape indicating that such glass-ceramics can be used as a basis for obtaining construction material. The synthesis of pressed samples of mixtures (T20 and T40) at 1080°C for 36 h produces glass-ceramics that have a high coefficient of sound attenuation, which indicates good acoustic insulating properties.*

**Keywords:** FFW; Zeolite tuff; Sintering; Glass-ceramics; Phase composition.

---

## 1. Introduction

Copper extraction, especially in the process of flotation enrichment and pyrometallurgical processing, generates waste materials that pollute the environment [1]. Flotation tailings and smelter slag dumps represent large areas of degraded land and are permanent sources of soil, water, and air pollution [1-4].

Recycling of industrial waste material is a frequent topic of numerous scientific papers, in which vitrification provides construction material of appropriate quality and desired properties [4-10]. Glass-ceramics is an attractive material that can have various applications, such as: building materials, ceramics for dishes, glass semiconductors for thermal insulation, optical materials [11-21], materials for orthopedic medicine [22], etc.

---

\*) Corresponding author: mcocic@tfbor.bg.ac.rs

Glass-ceramic materials have great application possibilities because their properties can be controlled, including strength, abrasion resistance, coefficient of thermal expansion [23,24]. The general process of obtaining glass-ceramics involves vitrification of silicate waste or a mixture of waste, followed by crystallization [22]. The synthesis of parent glass is an important step in the preparation of the final glass-ceramic material because the precursors and their percentage in the glass composition control the formation of crystalline phases [23].

Glass-ceramic materials obtained by vitrification of waste from the copper [6,10] and zinc industry [25] are chemically stable and have significantly better characteristics compared to traditional ceramics and natural building materials. For example, vitrified ash from the municipal solid waste incineration process (MSWI) has been successfully converted into strong and chemically stable porous glass-ceramics by a combination of alkaline activation and sintering [26].

High-strength lightweight glass-ceramics were obtained by sintering coal and clay tailings at 1370°C [11,27].

Waste galvanic sludge, aluminum slag, and glass were inactivated and incorporated into glass-ceramics by a sintering process to minimize or completely eliminate the risk of environmental pollution [19].

Sphene-based glass-ceramics ( $\text{CaTiSiO}_5$ ), which is prepared from a mixture of  $\text{CaCO}_3$ ,  $\text{TiO}_2$ , and  $\text{SiO}_2$  powders using vibro-grinding for homogenization, can be used to immobilize nuclear waste [23].

Basalt-based glass-ceramics (from the Vrelo deposit, Kopaonik) have a very fine and homogeneous structure, excellent physical and mechanical properties, chemical resistance, high resistance to wear and corrosion, and can replace metallic materials in metallurgical and mining equipment [28-36].

Direct sintering of iron-rich metallurgical slag from Belgium (KU Leuven) and recycled sodium-lime glass yielded lightweight glass-ceramics, with limited water absorption, mechanical properties comparable to those of lightweight porcelain tiles, and chemical stability [37].

The application and use of zeolite tuffs in construction (light building stone) have been known since ancient times [38]. In particular, clinoptilolite zeolite has a wider application in construction [38], as a pozzolan in cement production [39-43], as an additive for asphalt mixing and partial replacement of fillers [44], as an additive in the concrete mix [45,46], for obtaining lightweight concrete or as a thermal insulation material [47].

It was found that 5 % of ground zeolite (from Lyulinskoe deposit, Russia) with granulation of 5–10 mm increases the compressive strength of cement by 15 % in 7 days and 21 % in 28 days [42].

The addition of natural zeolites and fly ash (waste material obtained from thermal power plants) as an additive has a positive effect on the mechanical and physical properties of concrete [48].

Melting 30 % slag from copper flotation, 30 % blast furnace slag, and 40 % zeolite tuff in electric furnaces, in an air atmosphere, for 30 min at 1400°C, obtained a mixture of high crystallization, suitable for the production of glass-ceramics [10].

In addition, since the exchangeable cations in the zeolite structure ( $\text{Na}^+$ ,  $\text{K}^+$ ,  $\text{Ca}^{2+}$ , and  $\text{Mg}^{2+}$ ) are not toxic, zeolites are also tested as ion exchangers and adsorbents for use in wastewater treatment, reclamation of flotation tailings, adsorption of mycotoxins [49-51]. Also, the use of zeolite as an adsorbent in veterinary medicine [52] and the removal of heavy metals from industrial wastewater [53-55] is being studied.

Many studies cite zeolite as a cost-effective adsorbent because of its good metal-binding capacity, local availability in large quantities, simple operation technology, and avoidance of secondary pollution [54].

Zeolite tuff (Igroš near Brus, Serbia) in certain relations with FFW (RTB Bor, Serbia) can be used for the production of glass-ceramic material [4,18].

The previously published papers [18,34,56,58] present the basic and most important characteristics of the raw materials, as well as the production and characterization of glass-ceramics synthesized at different temperatures and different time intervals.

The results of additional research of starting materials (DTA FFW, tuff microscopy, IR tuff, XRPD tuff) and characteristics of glass-ceramics (crystal phase content, ultrasonic damping coefficient) presented in this paper complete the presentation of the possibilities of their application.

## 2. Materials and Experimental Procedures

The waste smelter slag flotation process has been described previously [34,56]. In the process of flotation of waste smelter slag, the tailings of the basic flotation are formed, which is the final flotation waste - FFW. A sample of FFW was taken before transport to the landfill.

The sample of zeolite tuff was taken from the deposit "Igroš - Vidojevići" (Serbia), located about 8 km east of Brus, and 3 km northeast of the river Rasina. Zeolite tuff is interstratified in the Miocene-Pliocene series of marly green clays that form the bottom and brown clays and sandstones that form the overburden. The layer of zeolite tuff is light gray to white, 1–4 m thick, with a general east-west extension and an average slope to the north at an angle of about 10 degrees [57]. Prior to analysis, the material was prepared by crushing and homogenizing.

The tests are divided into two parts. The first part included the characterization of starting materials: FFW and tuff. Their phase, chemical composition, and thermal properties (sintering, softening, and melting interval) are presented in previous works [34,58]. In order to better understand the type of crystal phases in sintered glass ceramics, DTA of FFW was performed. In order to identify fine-grained hydrated minerals - zeolites, which are part of the tuff, the infrared spectrum was recorded, then microscopy was performed (on a Leitz-orthoplan wetzlar microscope in transmitted light) and XRPD of tuff.

The phase composition of the samples was determined by X-ray powder diffraction analysis (XRPD). Diffractograms were obtained using a Siemens D500 diffractometer with  $\text{CuK}\alpha$  radiation ( $\lambda = 1,54184 \text{ \AA}$ ) and Ni-filters at a current of 20 mA and a voltage of 35 kV in the range of 5 - 85 degrees ( $2\theta$ ) with a step of 0.02 degree and an exposure of 0,5 s per step. The phase ratio was determined by Powder Cell (PCW) software using structural models of fayalite [59], magnetite [60], clinoptilolite [61], biotite [62], plagioclase [63], quartz [64], smectite [65] hematite [66] and maghemite [67].

The chemical composition of FFW was determined by X-ray fluorescence analysis (PANalytical AXIOS XRF Spectrometer). The microstructure of the synthesized glass-ceramics was obtained by Scanning Electron Microscopy (SEM) on an instrument of the JSM-6610 LV type, under high vacuum conditions. LaB6 filament was used as the electron source. Chemical analyzes of the samples were performed on an Energy Dispersion Spectrometer (EDS) of the X-Max Large Area Analytical Silicon Drift (Oxford) type, on polished samples using external standards. The samples were evaporated with carbon on a steamer type BALTEC-SCD-005. The thickness of the vaporized layer was 18 nm [34].

A modernized Chevenard Joumier Instrument A.D.A.M.E.L. was used for differential thermal analysis (DTA) of FFW. This instrument was equipped with a Pt - PtRh thermocouple and a computer system for data acquisition. T and dT data were collected by USB-2523 DAC board with a sampling rate of 1 Hz and a heating mode of 8 °C/min. In this way, 7350 values were collected in the temperature range from 20 to 1000°C. The reference material was  $\alpha\text{-Al}_2\text{O}_3$ . Interpretation of thermograms was performed on the basis of literature data [68].

Infrared spectroscopic analysis was performed by using a Perkin Elmer 597 spectrometer with the KBr pellet method in the region 200- 4000  $\text{cm}^{-1}$ .

The second part of the study included the determination of additional characteristics of glass-ceramics obtained by sintering samples, in the presence of a liquid phase from a mixture of FFW with tuff: T20 (20 % tuff, 80 % FFW) and T40 (40 % tuff, 60 % FFW) at 1260°C/7 h [34,58].

The glass-ceramic bodies (diameter 30 mm, thickness 20 mm) were synthesized at 1080°C for 36 h, by pressing FFW and mixtures of T20 and T40. Their characteristics were evaluated in a previously obtained paper [34] by measuring: Vickers hardness (measured with a durometer, by imprinting a small diamond pyramid with a square cross-section on the surface of the sample), density, speed of propagation of ultrasonic longitudinal waves, and exposure to thermal shock by successive heating of samples from 100 to 800°C and sudden immersion in water at room temperature. Before measuring the propagation rate of the ultrasound, the samples were dried to remove adsorbed moisture). Changes in the hardness and speed of ultrasound propagation were monitored after the thermal shock [34]. The volumetric mass before and after sintering and the damping coefficient of ultrasound before and after exposure to thermal shock were additionally measured in order to a full examination of the possibility of application of the synthesized glass-ceramics.

### 3. Results and Discussion

#### 3.1. Characterization of starting material

##### 3.1.1. Final flotation waste (FFW) characteristics

X-ray diffraction analysis of FFW powder identified two crystalline phases: fayalite ( $\text{Fe}_2\text{SiO}_4$ ) [59] and magnetite ( $\text{FeO}\cdot\text{Fe}_2\text{O}_3$ ) [60] and a significant amount of amorphous matter were observed, while chemical analysis revealed a high content of iron (III) oxide ( $\approx 52\%$ ) and silicon dioxide ( $\approx 34\%$ ), then about 5 %  $\text{Al}_2\text{O}_3$  and CaO, and about 1%  $\text{K}_2\text{O}$ , while the content of other oxides is below 1 % (Fig. 1).

The phase composition of FFW was calculated on the basis of X-ray diffraction analysis, chemical composition analysis and using theoretical, stoichiometric formulas of magnetite, and fayalite. The obtained values of phase content in FFW: fayalite ( $\approx 40\%$ ), magnetite ( $\approx 25\%$ ), and glass ( $\approx 35\%$ ) represent a significant basis for the production of glass-ceramics [34,58].

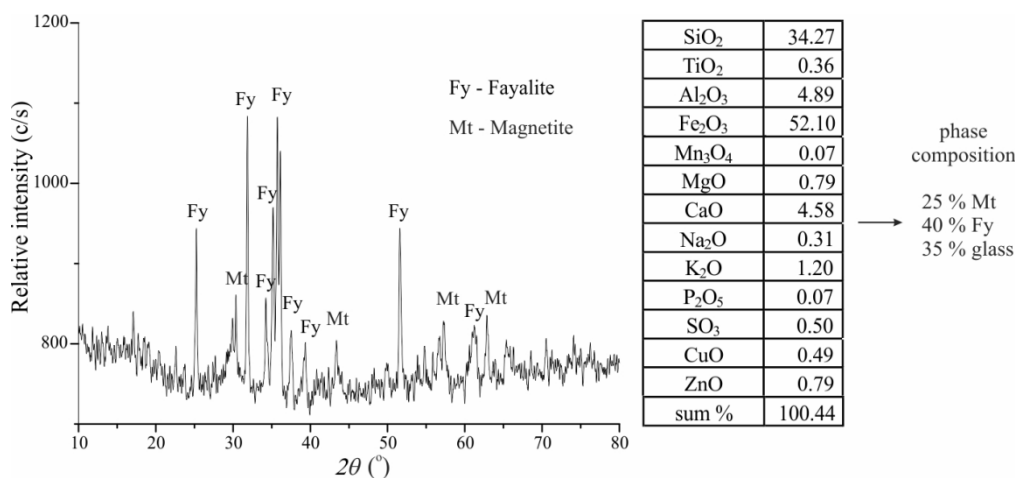


**Fig. 1.** X-ray powder diffraction diffractogram and chemical composition of FFW.

Possible phase transitions of FFW during the formation of glass-ceramics are partially defined by DTA analysis (Fig. 2). DTA analysis showed that as a consequence of the loss of adsorbed moisture at 110°C, a pronounced endothermic reaction occurs. An exothermic reaction occurs at 400°C as a consequence of the oxidation of magnetite to hematite  $\gamma$ -Fe<sub>2</sub>O<sub>3</sub> (on the grain surface). As a consequence of the oxidation of magnetite to hematite  $\gamma$ -Fe<sub>2</sub>O<sub>3</sub> (in the grain core), an exothermic reaction at 575°C also occurs [68]. At a temperature of 705°C, an exothermic reaction of the transition of  $\gamma$ -Fe<sub>2</sub>O<sub>3</sub> to  $\alpha$ -Fe<sub>2</sub>O<sub>3</sub> occurs [58].

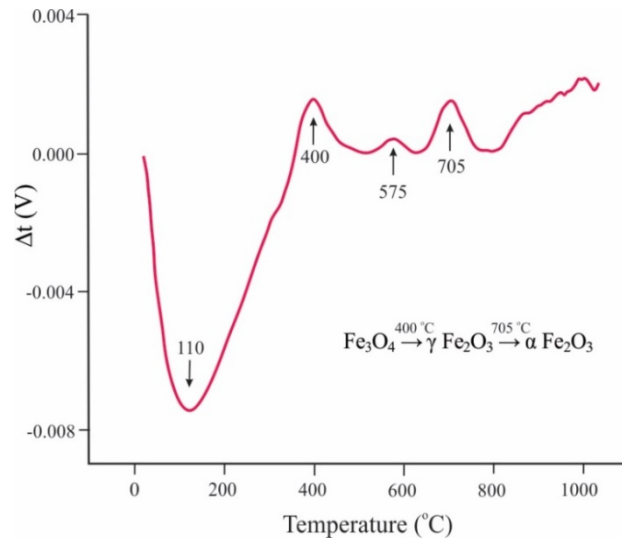


**Fig. 2.** DTA diagram of FFW.

### 3.1.2. Characteristics of zeolite tuff

Tuff 'Igroš - Vidojevići' (Fig. 3a) is built mainly of fine-grained amorphous volcanic ash, which is largely zeolitized, i.e. transformed into clinoptilolite. In addition to clinoptilolite, biotite leaves, plagioclase grains (Fig. 3b) and quartz appear in the examined tuff, and amphibole and zircon appear in subordinate quantities. Plagioclase is well preserved with developed polysynthetic lamellae and sometimes pronounced zonal structure. Quartz grains are sparse, anhedral, broken, with frequent undulatory eclipses. The grain size of the listed minerals belongs to the class above 0.06 mm [58].

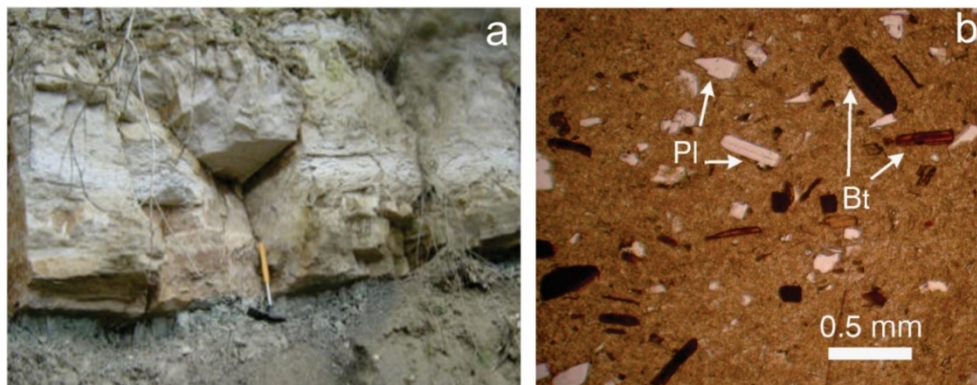


**Fig. 3.** a) Tuff outgrowth 'Igroš - Vidojevići'; b) micrograph of tuff (Pl - plagioclase, Bt - biotite).

X-ray diffraction analysis confirmed the presence of zeolite - clinoptilolite [62], then biotite [62], plagioclase [63] and quartz [64]. In addition to these phases, X-ray diffraction analysis also determined the presence of smectite [65] (Fig. 4). The high content of total water in the chemical analysis of tuff indicates that clinoptilolite is the dominant mineral phase. Although CaO and Na<sub>2</sub>O partly participate in the construction of plagioclase, the relatively high content of CaO (> 5 %) in relation to Na<sub>2</sub>O (< 1 %) (Fig. 4) indicates that Ca-clinoptilolite is most likely present.

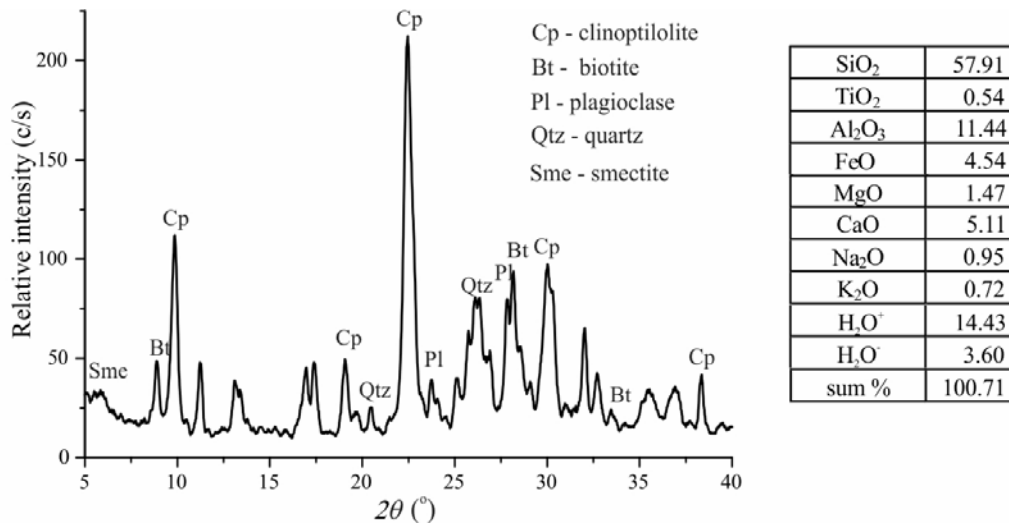


**Fig. 4.** X-ray powder diffraction diffractogram and chemical composition of tuff.

The presence of clinoptilolite was also confirmed by infrared spectroscopy. A series of absorption maxima on the spectrum shown (Fig. 5) correspond to clinoptilolite. The bands at 3595 cm<sup>-1</sup> and 3427 cm<sup>-1</sup> originate from the valence vibrations (OH) of the group, and the bands at 1630 cm<sup>-1</sup> from H<sub>2</sub>O molecules in the variable structural positions characteristic of zeolites. Absorption maxima between 800 and 1300 cm<sup>-1</sup> are due to vibrations of the silicate lattice.

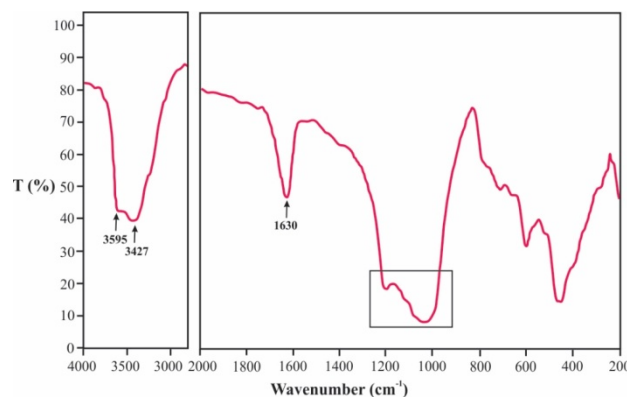


**Fig. 5.** IR spectra of investigated tuff.

### 3.1.3. Thermal characteristics of raw materials and raw material mixtures

The results of previously performed tests of thermal characteristics of starting materials determined by thermal microscope at 12 °/min indicate that tuff has a higher

temperature of the beginning and end of sintering, but less volume change (5.4) and significantly narrower sintering interval (20) compared to FFW [34,58].

Due to dehydration of clinoptilolite (which is the dominant mineral in tuff) at 240 - 350°C, shrinkage occurs (2 %). The large contraction caused by the collapse of the clinoptilolite structure occurs in the temperature range of 850 to 950°C producing a shrinkage of 31.5 %. Structural collapse is absent in mixtures of T20 and T40, which is a consequence of the development of the liquid phase from FFW which begins at the matching temperature by occluding/closing/ preventing clinoptilolite grains. This blocks the emptying of structural channels and stops structural collapse. The reaction of FFW particles with tuff particles dominated by clinoptilolite does not allow its structural collapse. At T40, a minimal contraction (-0.7 %) at 850°C was observed, indicating the onset of the collapse of the clinoptilolite structure. The beginning of sintering in both mixtures is at the temperature of the end of sintering FFW (1080°C). The end of sintering at T20 and T40 coincides with the sintering end temperature of pure tuff (1160°C). With increasing tuff content, there are no temperature changes [34,58].

### 3.2. Phase and chemical composition of synthesized glass-ceramics

Thermal treatment of mixtures of FFW with tuff, ie samples: T20 (20 % tuff, 80 % FFW) and T40 (40 % tuff, 60 % FFW), up to a temperature of 1260°C for a period of 7 hours, synthesized glass-ceramics [34,58]. X-ray diffraction analysis in both synthesized glass-ceramics (T20 and T40) identified hematite [66], maghemite [67] and magnetite [60] (Fig. 6), which indicates a structural variation of iron oxides [34,58]. In addition to iron oxides, a glassy phase also occurs in glass-ceramic samples T20 and T40.

A significant difference in the chemical composition of the synthesized glass-ceramic T20 in relation to T40 is in the higher content of iron (III) oxide and lower content of SiO<sub>2</sub>, Al<sub>2</sub>O<sub>3</sub> and CaO (Fig. 6).

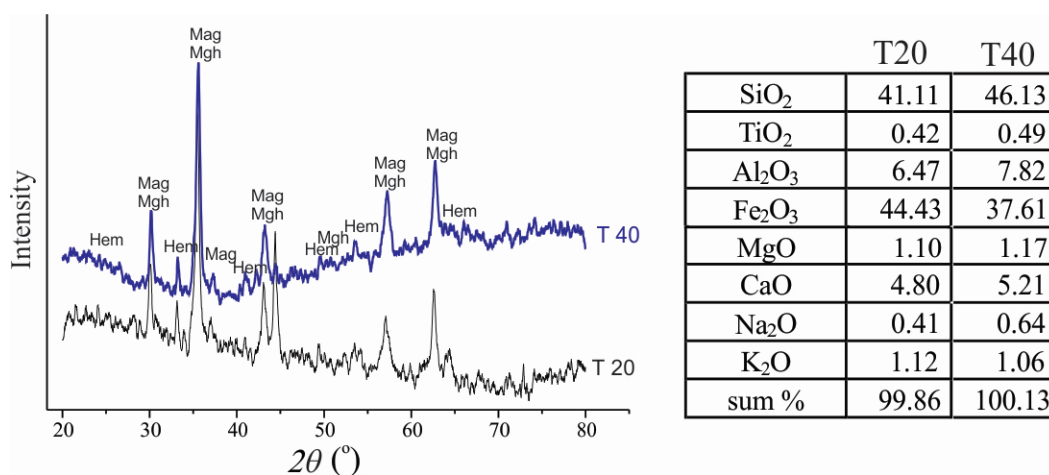


**Fig. 6.** X-ray powder diffraction diffractogram and chemical analyses of the obtained glass-ceramics.

The crystalline phase, i.e. iron oxides in the examined glass-ceramics (T20 and T40) identified by X-ray diffraction analysis as magnetite, hematite and maghemite (Fig. 6) mainly appear in the form of dendritic aggregates (Fig. 7a,c). Individual crystals are most morphologically reminiscent of hematite because they appear in the form of subhedral rhombohedral crystals (Fig. 7b,d). A similar glass microstructure has been described by Romero & Rincon [7].

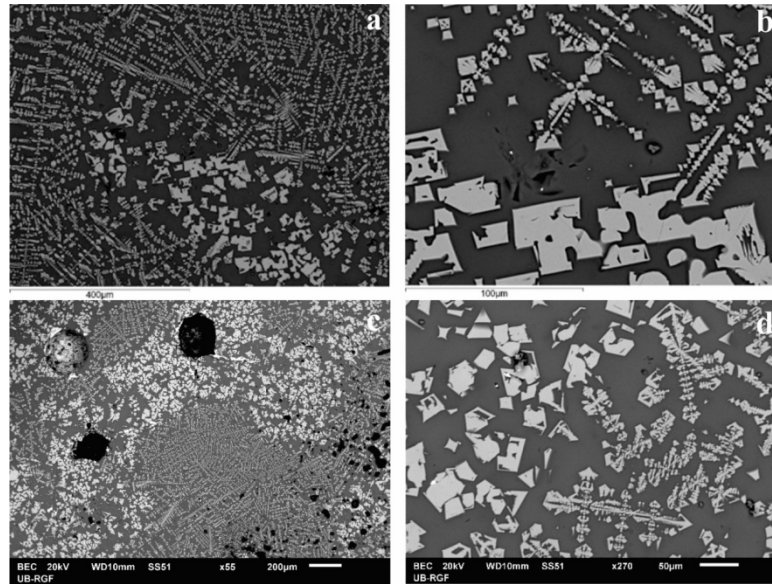


**Fig. 7.** Microstructure of synthesized glass-ceramics: a) dendritic aggregates of the crystalline phase in glass-ceramics (T20), b) detail of dendrites and individual crystals (T20), c) dendritic aggregates of the crystalline phase in glass-ceramics (T40), d) detail of dendrites and individual crystals (T40).

The crystal content in the synthesized glass-ceramics was determined by integration using digital image analysis based on the surface they occupy in the observed cross-section. T20 is 32.3 % (Fig. 8 a,b) and T40 is 23.3 % crystals (Fig. 8 c,d).

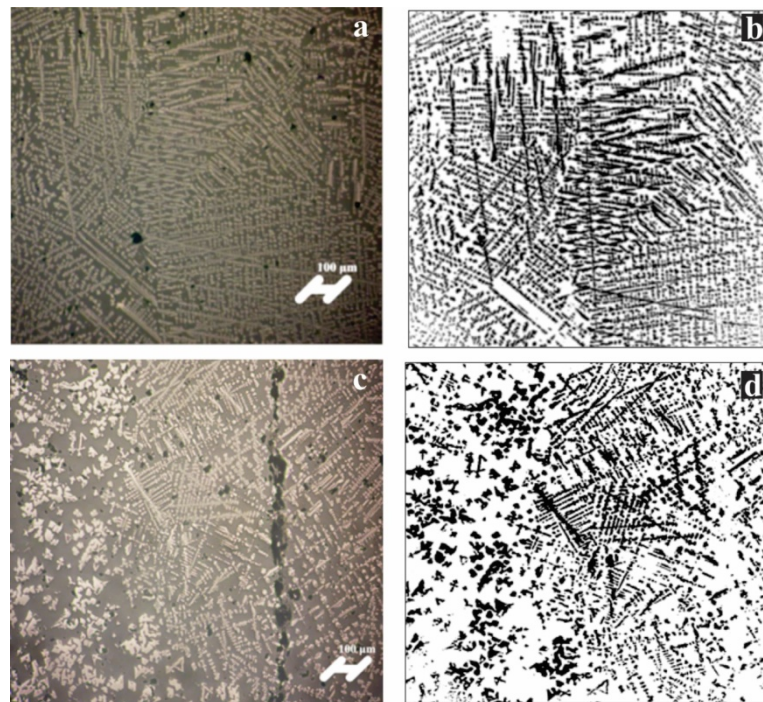


**Fig. 8.** a) integrated surface of glass-ceramics T20, b) computer simulation of integrated surface T20, c) integrated surface of glass-ceramics T40, d) computer simulation of integrated surface T40.

### 3.3. Mechanical properties of synthesized glass-ceramics

In a cylindrical mold (diameter 30 mm, thickness 20 mm), lozenges (from 35 g of the FFW, T20, and T40 sample) in the form of a cylinder (Fig. 9a) were made and pressed at a pressure of 70 MPa [34]. Glass-ceramic bodies were synthesized at 1080°C for 36 h the characteristics of which were determined by measuring: volumetric mass, ultrasonic propagation velocity and ultrasonic damping coefficient before and after exposure to thermoshock at different temperatures.

The volumetric masses of samples FFW, T20, and T40 before sintering were 2.7, 2.1, and 1.8 while after sintering they were 3.1, 2.4, and 2.5, respectively (Fig. 9a). The percentage of shrinkage in FFW is 13 % (which is in accordance with the results of thermal tests), and in mixtures, with tuff, it is about 12 %.

The results of the propagation velocity of ultrasonic longitudinal waves (Fig. 9b) show that the samples have velocities in the domain of compact materials (glass 3600 to 6100, concrete 2500 to 5000, cast iron 4410 m/s): FFW (4500 m/s), T20 (4150 m/s) and T40 (4100 m/s) [34]. In FFW, the speed of ultrasound decreases relatively slowly to the temperature of thermal shock at 400°C. Above this temperature, a sudden drop in the speed of ultrasound is observed, which indicates the appearance of discontinuities in the structure (cracks, fissures). In the T40 sample, a decrease in velocity is observed at a temperature of 200°C, and in the T20 already at 100°C, after which it decreases linearly towards a temperature of 800°C (Fig. 9b) [34].

The attenuation coefficient of ultrasound is higher in samples T20 and T40 compared to FFW (Fig. 9c). This speaks of elastic properties, as well as the texture of the material, where the size and distribution of pores and other discontinuities caused by thermal shock, produce ultrasonic signal scattering, ie amplitude reduction. High damping coefficients indicate good acoustic insulating properties of the material. On the other hand, high damping coefficients indicate weaker mechanical properties (pressure resistance, bending) due to the appearance of cracks.

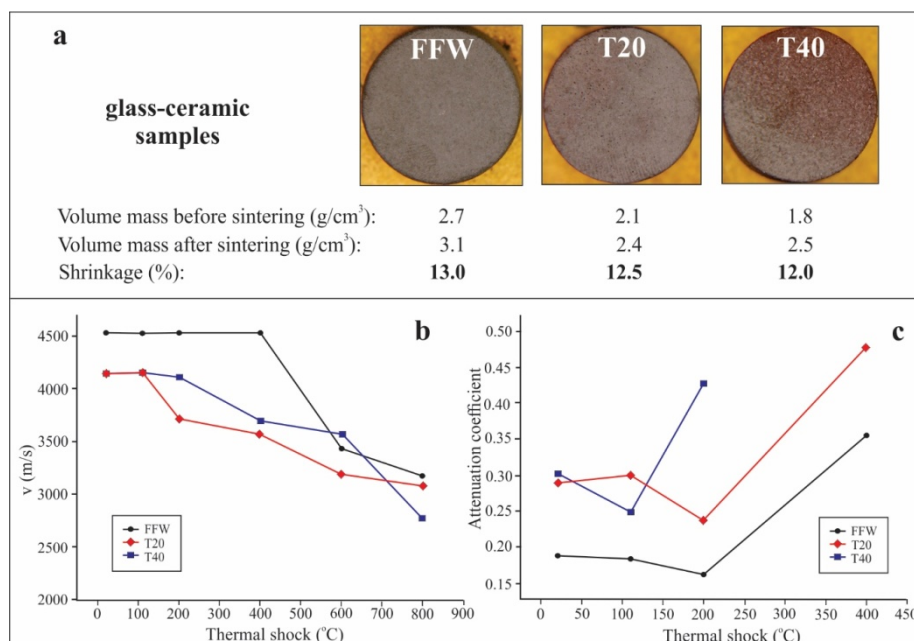


**Fig. 9.** Mechanical characteristics of FFW, T20, and T40 glass-ceramics a) bulk density before and after sintering and shrinkage b) propagation velocities of ultrasonic longitudinal waves of samples exposed to thermoshock, c) ultrasonic damping coefficient.

### 3.4. Comparison of FFW glass-ceramic characteristics with T20 and T40 glass-ceramics

It should be mentioned that with increasing sintering temperature and time, the crystal content in FFW glass-ceramics increases. For example, if the sintering conditions are 1100 °C/4h, the crystal phase content is about 27 %, under 1150 °C/4h conditions the crystal content is about 32 %, while by synthesis at 1480 °C/6h the crystal phase content reaches 44 %. The morphological characteristics of the crystal phase also change, from anhedral to rarely subhedral forms at lower synthesis temperatures to almost completely regular, euhedral crystals in synthesis at higher temperatures [34]. This confirms that by changing the heat treatment conditions and cooling regime, the microstructure and properties of the product can be controlled, i.e. glass-ceramic material with predetermined properties can be produced.

In general, FFW glass-ceramics is a "bubble" structure, as a consequence of gas emanation due to thermal treatment. It is made of hematite as a crystalline phase and a glassy phase, and due to its "hollow" structure, it has good thermal insulation properties, i.e. it is an excellent thermal insulator [34].

Glass-ceramics obtained from mixtures of T20 and T40 also consist of a glassy phase and a crystalline phase, but the crystalline phase is represented not only by hematite but also by other iron oxides, maghemite, and magnetite, which occur in the form of individual subhedral to euhedral crystals and/or in the form of acicular dendrites. The crystal content in the synthesized T20 and T40 glass-ceramics approximately corresponds to the crystal content in FFW glass-ceramics synthesized at lower temperatures (up to 1150°C): T20 - about 32 % and T40 - about 23 % (Fig. 8). In some crystals in these glass-ceramics, chemical zonation is observed, which refers to the distribution of Fe.

The data obtained by Vickers hardness [34] single out sintered FFW as a very hard material, with values up to 10800 MPa. The high hardness is primarily affected by the high content of iron oxide crystals (hematite) that are formed in the sintering process. Under the action of thermal shock, the hardness of FFW glass-ceramics drops sharply (from 10800 to 1730 MPa). Minor changes in hardness were found only at lower temperatures of thermal shock (up to 600°C), which is why this glass-ceramic could be used for the needs of building ceramics where resistance to thermal shock of 200 and 400°C is required.

On the other hand, although glass-ceramics obtained from mixtures of T20 and T40 have a significantly lower hardness (T20 - 2491 MPa, T40 - 1157 MPa), they do not suffer a large change in hardness due to thermal shock at higher temperatures than glass-ceramic FFW [34]. This is most likely due to the different bond strengths between the sintered particles in the samples of different compositions. The damping coefficient of ultrasound of the tested samples of glass-ceramics at room temperature is even over 30 % higher in glass-ceramics T20 and T40 in relation to glass-ceramics FFW. This tendency continues at higher temperatures (Fig. 9c). Therefore, mixtures with tuff would find their application in the field of building ceramics, especially in areas where good sound insulation is required. Finally, it should be emphasized that according to the data obtained in [1,2,34] in the areas around the industrial plant in Bor (Serbia), the total amount of waste smelter slag disposed of in the landfill is about 16 million tons. This now significantly increased deposited material should certainly be used, both for economic and environmental reasons. One of the ways to use them is precisely synthesized glass-ceramic materials (pure FFW and mixtures of T20 and T40) which would certainly find their significant application in various building materials.

## 4. Conclusion

Thermal treatment of mixtures of FFW and zeolite tuff T20 (20 % tuff, 80 % FFW) and T40 (40 % tuff, 60 % FFW) to a temperature of 1260°C over a period of 7 h, synthesized

glass-ceramics made of iron oxide crystals (maghemite, magnetite, and hematite) and glass (with an approximate ratio of phases 32/68 (T20) and 23/77 (T40), respectively). Crystals most often appear in the form of dendritic aggregates, which represent a kind of reinforcement in glass and improve the general mechanical properties of glass-ceramics.

FFW glass-ceramics could be used for the needs of building ceramics where thermal shock resistance up to 200°C is required. (above 200°C, there is an increase in structural discontinuities, which can be seen from the large attenuation of the ultrasound signal.) Mixtures with tuff would also find their application in the field of building ceramics, especially in areas where good sound insulation is required. The relatively small shrinkage of the synthesized material (about 7 %) allows reliable control when designing a given shape. This indicates that it can be used as a basis for obtaining construction materials.

## Acknowledgments

The research presented in this paper was done with the financial support of the Ministry of Education, Science and Technological Development of the Republic of Serbia, within the financing of scientific research work at the University of Belgrade, Technical Faculty in Bor, according to the contract number 451-03-9 / 2021- 14/200131.

## 5. References

1. M. Dimitrijevic, A. Kostov, V. Tasic and N. Milosevic, *J. Hazard. Mater.*, 164 (2009) 892.
2. R. Stanojlović, Z. Stirbanović J. Sokolović, *JMM*, 44 (2008) 44.
3. G. Bogdanović, M. Trumić, Maja Trumić, D. Antić, *ROR*, 4 (2011) 37.
4. Cocić M., Application of the flotation waste from the RTB Bor for glass-ceramics, PhD thesis. Faculty of Mining and Geology, University of Belgrade, Belgrade, 2012.
5. B. Gorai, R.K. Jana, Premchand, *Resources, Conserv. Recycling*, 39 (2003) 299.
6. S. Coruh, O. Nuri Ergun and T. Cheng, *Waste Manage. Res.*, 24 (2006) 234.
7. M. Romero and J. Ma. Rincon, *J. Eur. Ceram. Soc.*, 18 (1998) 153.
8. G. Scarinci, G. Brusatin, L. Barbieri, A. Corradi, I. Lancellotti, P. Colombo, S. Hreglich and R. Dalligna, *J. Eur. Ceram. Soc.*, 20 (2000) 2485.
9. A. Karamanov, G. Taglieri, M. Pelino, *J. Am. Ceram. Soc.*, 82 (1999) 3012.
10. A. Karamanov, M. Aloisi and M. Pelino, *J. Hazard. Mater.*, 140 (2007) 333.
11. D. Wei1, H.-Y. He, *Sci. Sinter.*, 51 (2019) 285.
12. E. Tutić, M. Jovanović, A. Mujkanović, *Sci. Sinter.*, 48 (2016) 247.
13. P. Parra, M. Vlasova, P. A. M. Aguilar, T. Tomila, *Sci. Sinter.*, 49 (2017) 207.
14. O. R. K. Montedo, I. T. Alves, C. A. Faller, F. M. Bertan, D. H. Piva, R. H. Piva, *Mater. Res. Bull.*, 72 (2015) 90.
15. A. Mirza, M. Riaz, Hussain, F. Bashir, *J. Alloy. Comp.*, 726 (2017) 348.
16. V. Karayannis, A. Moutsatsou, A. Domopoulou, E. Katsika, C. Drossou, A. Baklavariadis, *J. Build. Eng.*, 14 (2017) 1.
17. A. Terzić, N. Đorđević, M. Mitrić, S. Marković, K. Đorđević, V. B. Pavlović, *Sci. Sinter.*, 49 (2017) 23.
18. M. Cocić, B. Matović, M. Posarac, T. Volkov- Husović, J. Majstorović, V. Tasić, S. Dević, N. Vusović, *Sci. Sinter.*, 49 (2017) 139.
19. I. Krstić, S. Zec, V. Lazarević, M. Stanisavljević, T. Golubović, *Sci. Sinter.*, 50 (2018) 139.
20. O. R. K. Montedo, C. A. Faller, F. M. Bertan, J. Justin, R. H. Piva, D. H. Piva, *Ceram. Int.*, 43, 15 (2017) 11864.

21. G. Sharma, S.K. Arya, K. Singh, *Ceram. Int.*, 44, 1 (2018) 947.
22. Nur F. B. P. et al., *Sci. Sinter.*, 51(2019) 377.
23. J. Maletaškić, B. Todorović, M. Gilić, M. Marinović Cincović, K. Yoshida, A. Gubarevich, B. Matović, *Sci. Sinter.*, 52 (2020) 41.
24. D. U. Tulyaganov, S. Agathopoulos, J. M. Ventura, M. A. Karakassides, O. Fabrichnaya, J. M. F. Ferreira, *J. Eur. Ceram. Soc.*, 26 (2006) 1463.
25. M. Pelino, *Waste Manage.*, 20 (2000) 561.
26. P. R. Monich, F. Dogrul, H. Lucas, B. Friedrich and E. Bernardo, *Detritus*, 08 (2019) 101.
27. W. Dang & H.-Y. He, *J. Asian Ceram. Soc.*, 8 (2020) 365.
28. M. Pavlović, M. Dojčinović, R. Prokić-Cvetković, Lj. Andrić, *Sci. Sinter.*, 51 (2019) 409.
29. M. Pavlović, M. Dojčinović, Lj. Andrić, D. Radulović, *J Min Metall Sect A*, 55 (2019) 37.
30. B. Matović, S. Bošković, *J. Serb. Chem. Soc.*, 68 (6) (2003) 505.
31. M. Cocić, M. Logar, B. Marović, V. Poharc-Logar, *Sci. Sinter.*, 42 (2010) 383.
32. Z. Nikolić, K. Shinagawa, *Sci. Sinter.*, 49 (2017) 1.
33. Parra Parra, M. Vlasova, P. Antonio Márquez Aguilar, T. Tomila, *Sci. Sinter.*, 49 (2017) 207.
34. M. Cocić, M. Logar, S. Erić, V. Tasić, S. Dević, S. Cocić, B. Matović, *Sci. Sinter.*, 49 (2017) 431.
35. Lj. Kostić-Gvozdrenović, R. Ninković, *Inorganic Chemical Technology, Faculty of Technology and Metallurgy, Belgrade, 1997 (In Serbian)*
36. Proceedings: R. Simic, N.Gilic, in: 'Conference Rock' Arandelovac, 2000, p. 150-155.
37. I. Ponsot, R. Detsch, A. R. Boccaccini & E. Bernardo, *Adv. Appl. Ceram.*, 114 (2015) 17.
38. Margeta, A. Farkaš and Z. Glasnović, *Građevinar*, 63 (2011) 1009.
39. Ahmadi and M. Shekarchi, *Cement Concrete Comp.*, 32 (2010) 134.
40. Bilim, *Constr. Build. Mater.*, 25 (2011) 3175.
41. V. Sasnauskas, G. Rinkevičius, D. Martinavičius, D. Vaičiukynienė and E. Ivanauskas, *JSACE* 2, 11 (2015).
42. T N Smorodinova, M K Kotvanova, I A Sologubova, S S Pavlova, *IOP Conference Series: Materials Science and Engineering*, 913 (2020) 032039.
43. B. Liguori, F. Iucolano, B. de Gennaro, M. Marroccoli, D. Caputo, *Constr. Build. Mater.* 99 (2015) 272.
44. A. Wozzuk, M. Wróbel, W. Franus, *Materials*, 13 (2020) 19.
45. A. Ramezani-pour, A. Kazemian, M. Sarvari and B. Ahmadi, *J. Mater. Civ. Eng.*, 25, (2013) 589.
46. Karakurt, H. Kurama, and I. Bekir Topçu, *Cement Concrete Comp.*, 32, (2010) 1.
47. S. Djambazov, A. Yoleva, P. Chervenliev and A. Georgiev, *J. Chem. Technol. Metall.*, 50 (2015) 520.
48. K. Güçlüer, O. Günaydın, O. Ünal, S. Bilen, *JMEST*, 3 (2016) 4119.
49. A. Daković, M Tomašević-Čanović, V. Dondur, A. Vujaković, P. Radošević, *J. Serb. Chem. Soc.*, 65 (2000) 715.
50. A. Daković, M. Tomašević-Čanović, V. Dondur, G. E. Rottinghaus, V. Medaković, S. Zarić, *Colloid Surface B*, 46 (2005) 20.
51. M. Kragović, A. Daković, Ž. Sekulić, M. Trgo, M. Ugrina, J. Perić, G. Diego Gatta, *Appl. Surf. Sci.*, 258 (2012) 3667.
52. F. A. Mumpton, P. Fishman, *J. Anim. Sci.*, 45 (1977) 1188.

53. N. Vukojević Medvidović, J. Perić, M. Trgo, Sep Purif Technol., 49 (2006) 237.
54. S. Milićević, M. Vlahović, M. Kragović, S. Martinović, V. Milošević, I. Jovanović, M. Stojmenović, Minerals 10 (2020) 753.
55. V. Kašić, S. Mihajlović, D. Životić, V. Simić, J. Stojanović, Ž. Sekulić, M. Kragović, Hem. Ind., 72 (2018) 29.
56. Cocić M., Logar M., Matović B., Dević S., Volkov-Husović T., Cocić S., Tasić V., Sci. Sinter., 48 (2016) 197.
57. J. Obradović, Geol. Anali Balk. Pol., XLI, (1977) 293-302.
58. M. Cocić, M. Logar, Section lectures, XIII International Mineral Processing and Recycling Conference, Belgrade, Serbia, 8 - 10 May 2019.
59. J. R. Smyth, Am. Mineral., 60 (1975) 1092.
60. E. Fleet, Acta Crystallogr. B, 37 (1981) 917.
61. Armbruster T., Gunter, M.E., Am. Mineral., 76 (1991) 1872.
62. Brigatti M F, Davoli P, Am. Mineral., 75 (1990) 305.
63. W. Horst, T. Tagai, M. Korekawa, H. Jagodzinski, Z. Kristallogr. 157 (1981) 233.
64. W. H. Zachariasen and H. A. Plettinger, Acta Cryst. 18, (1965) 710.
65. Brigatti, M.F. Clay Minerals: 18, (1983) 177.
66. E. N. Maslen, V. A. Streltsov, N. R. Streltsova and N. Ishizawa, ASBSD, 50 (1994) 435.
67. Greaves, J. Solid State Chem., 49 (1983) 325.
68. Ivanova V. P, Kasatov B. K., Krasavina T. N., Rozinova E. L., Kolterman&Miller, 'Thermal analysis of minerals and ore minerals' (1963).

**Сажетак:** Рад се бави карактеристикама синтетизоване стаклокерамике добијене синтеровањем смеше финалног флотационог отпада (FFW) са туфом на 1260°C у трајању од 7 сати, након чега је уследило жарење пресованих узорака на 1080 °C у трајању од 36 сати. Експерименти су рађени у циљу проналажења могућности за валоризацију отпадног материјала (FFW). Термичком обрадом смеша Т20 (20 % туфа, 80 % FFW) и Т40 (40 % туфа, 60 % FFW) на температуру од 1260 °C у трајању од 7 сати, добија се стаклокерамика дендритске структуре. Синтетизована стаклокерамика се састоји од две фазе: кристала оксида гвожђа (магемит, магнетит и хематит) и стакла са приближним односом фаза 32/68 (Т20) и 23/77 (Т40), респективно. Релативно мало скупљање синтетизованог материјала (до 7 %) омогућава поуздану контролу при пројектовању датог облика што указује да се таква стаклокерамика може користити као основа за добијање грађевинског материјала. Синтезом пресованих узорака смеша (Т20 и Т40) на 1080 °C у трајању од 36 сати добија се стаклокерамика која има висок коефицијент пригушења звука, што указује на добре акустично изолационе особине.

**Кључне речи:** FFW; зеолит туф, синтеровање, стаклокерамика, фазни састав.

© 2022 Authors. Published by association for ETRAN Society. This article is an open access article distributed under the terms and conditions of the Creative Commons — Attribution 4.0 International license (<https://creativecommons.org/licenses/by/4.0/>).

